Controlled manipulation of elastomers with radiation: Insights from multiquantum nuclear-magnetic-resonance data and mechanical measurements

A. Maiti,* T. Weisgraber, L. N. Dinh, R. H. Gee, T. Wilson, S. Chinn, and R. S. Maxwell
Lawrence Livermore National Laboratory, Livermore, California 94551, USA
(Received 19 October 2010; revised manuscript received 3 January 2011; published 17 March 2011)

Filled and cross-linked elastomeric rubbers are versatile network materials with a multitude of applications ranging from artificial organs and biomedical devices to cushions, coatings, adhesives, interconnects, and seismic-isolation, thermal, and electrical barriers. External factors such as mechanical stress, temperature fluctuations, or radiation are known to create chemical changes in such materials that can directly affect the molecular weight distribution (MWD) of the polymer between cross-links and alter the structural and mechanical properties. From a materials science point of view it is highly desirable to understand, affect, and manipulate such property changes in a controlled manner. Unfortunately, that has not yet been possible due to the lack of experimental characterization of such networks under controlled environments. In this work we expose a known rubber material to controlled dosages of γ radiation and utilize a newly developed multiquantum nuclear-magnetic-resonance technique to characterize the MWD as a function of radiation. We show that such data along with mechanical stress-strain measurements are amenable to accurate analysis by simple network models and yield important insights into radiation-induced molecular-level processes.

DOI: 10.1103/PhysRevE.83.031802 PACS number(s): 61.41.+e, 61.80.−x, 62.20.−x, 76.60.−k

I. INTRODUCTION

Even in matured materials fields such as elastomeric rubber and foam [1–3], it is important to look for new ways to manipulate properties. For instance, intense radiation (which is often used to sterilize biomedical devices [4]) is known to affect such materials [5–7] through the creation of new cross-links, breaking (scission) of covalent bonds, and modification of the polymer-filler interface. It would be technologically significant to utilize such changes and manipulate properties in a controlled way.

In spite of great advances in the statistical network theories [8,9] and insightful molecular/bead-spring-level simulations [10], understanding and manipulating materials properties of rubber can be possible only through a more detailed knowledge of the chemical and structural relaxation processes of the network. For instance, bond-scission phenomena under mechanical stress can trigger structural relaxation that can result in nontrivial feedback effects [11]. Probing of such details necessitates controlled experiments in which both the environment and the materials response can be characterized to a high degree of quantitative accuracy.

In this paper we subject a network silicone rubber material to relatively well-controlled ionizing radiation and use an array of experimental techniques to measure the stress-strain response, permanent set, and molecular weight distribution (MWD) between cross-links or entanglement junctions/restraints. We show how a simple network model allows an accurate quantitative interpretation of the mechanical data and yields a net rate of molecular-scale cross-linking/scission processes as a function of radiation. Finally, we incorporate such rates into a mesoscopic network model in an attempt to simulate the radiation-induced evolution of the MWD.

II. STRESS-STRAIN RESPONSE

For concreteness we chose a specific silicone elastomer, TR-55, for our study. It is a commercial rubber manufactured by Dow Corning, consists primarily of polydimethylsiloxane (PDMS), and incorporates roughly 30 wt% of silica filler. Thin samples (0.1 mm × 10 mm × 40 mm) were exposed to γ radiation from a Co-60 source (1.4 MeV, 0.5 Mrad/h dose rate) as a convenient, controllable degradation pathway. The samples were irradiated in a nitrogen atmosphere until the desired dosage was reached, and then subjected to mechanical analysis (Fig. 1) using a TA Instruments ARES LS-2 rheometer in torsion rectangle geometry. Measurements were made in the dynamic oscillatory shear mode at room temperature using a frequency of 1 Hz (6.28 rad/s). Strain was systematically incremented from the starting value (0.1%) to the end value (10%) using logarithmic spacing.

In order to model the stress-strain response of Fig. 1 the rubber material was treated as nearly incompressible. Over the years, various materials models have been developed to describe the mechanical behavior of incompressible rubber under compressive or tensile strain. The simplest of these is the neo-Hookean model [9,12], defined by the stress response function:

$$\sigma(\lambda) = G(\lambda^2 - 1/\lambda), \tag{1}$$

where σ is the (true) stress under a uniaxial stretch ratio λ ($\lambda = 1$ corresponding to the initial equilibrium state of no deformation). In Eq. (1) G is the shear modulus that is proportional to ν_0, the volume density of chain segments between cross-links (and other physical restraints) with the proportionality constant depending on the details of the network (i.e., bond coordination of the junctions, the fraction and nature of fillers, etc.). The best fits of the experimental data (symbols) in Fig. 1 by Eq. (1) yield the experimental shear modulus (G), plotted in Fig. 2 (symbols) as a function of radiation dosage D, along with errors due to sample-to-sample variation. The fit to the stress-strain response of the virgin material (Fig. 1 inset) yields a shear

*amaiti@llnl.gov

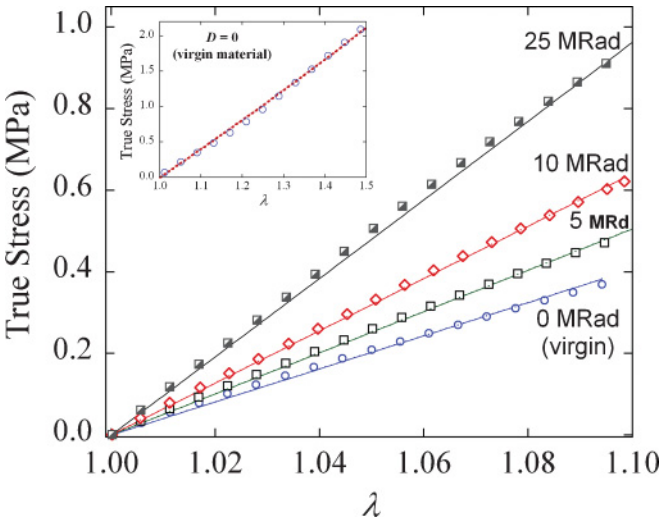

FIG. 1. (Color online) Stress-strain response of TR-55 subjected to different radiation dosages. Data are limited to stretch ratio (λ) of 1.1 or less. Experimental data (symbols) are displayed along with fits (lines) using the neo-Hookean model, Eq. (1), in text. Inset: Stress-strain response of the virgin material ($D = 0$) up to larger stretches ($\lambda \leqslant 1.5$) along with the neo-Hookean fit (dashed line) with $G = 1.35$ MPa.

modulus of $G_0 = 1.35$ MPa. Figure 2 shows that the shear modulus G increases, almost linearly, as a function of radiation (within our maximum dosage of 25 Mrad), implying a net increase in chain-segment density proportional to D.

III. PERMANENT SET MEASUREMENTS

As a consistency check, and also to gain possible insight into the relative importance of bond scission versus cross-linking events, a second set of experiments were performed in which several samples were irradiated *while* being under pre- constant tensile strain ($\lambda_1 = 1.20, 1.47, 1.67, 1.84$). Upon reaching the desired dosage, the samples were removed from the irradiation chamber, released from tensile strain, and allowed to relax at ambient conditions for a week. The relaxed samples were then

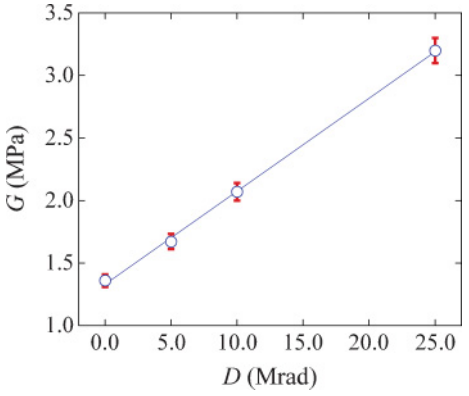

FIG. 2. (Color online) A plot of the shear modulus (G) from neo-Hookean fits to the data in Fig. 1 as a function of radiation dosage (D). Errors bars in G are due to sample-to-sample variation. The solid line is a linear fit to the data.

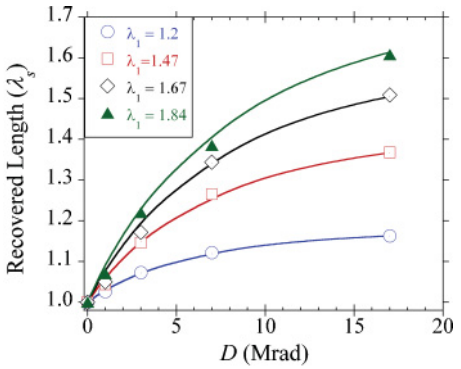

FIG. 3. (Color online) Permanent set data for TR-55 (expressed as recovered length (λ_s)) as a function of radiation dosage for different values of tensile stretch ratios (λ_1) at which the material is subjected to radiation. Solid lines are theoretical results using λ_1-independent f_{eff} (solid curve in Fig. 4 (top) below) in Eq. (5).

measured for the new equilibrium length, called the recovered length λ_s (symbols in Fig. 3), which is expressed as a ratio of the original (i.e., pre-exposure) equilibrium length [13]. As shown in Fig. 3, λ_s increases as a function of both λ_1 and the radiation dosage D [14].

IV. TOBOLSKY TWO-STAGE NETWORK MODEL

For a quantitative interpretation of Fig. 3, we adopt a two-stage independent network model originally proposed by Tobolsky [15], in which the rubber consists of (1) the original network at an equilibrium length of 1 (i.e., zero strain), a fraction of which gets *modified* by radiation (either through cross-linking or through bond scission), and (2) a new network created by radiation-induced cross-linking at an equilibrium length of λ_1. For concreteness of analysis let us assume an initial chain-segment density of ν_0, a fraction f_{mod} of which gets modified by radiation. Let us also assume that the new network has a chain-segment density ν_1, which as a fraction of the original chain density can be expressed as $\nu_1 = f_{xl}\nu_0$. In the presence of bond scission (and λ_1 different from 1), there is an additional feedback effect (due to physical network relaxation) in which a part Φ of the new network (called the transfer function) relaxes back into the original network. In this case, the *effective* number of chain-segment density in the two networks become [10] $\nu_0(1 - f'_{\text{mod}})$ and $\nu_0 f'_{xl}$, respectively, where $f'_{\text{mod}} = f_{\text{mod}} - \Phi f_{xl}$ and $f'_{xl} = (1-\Phi) f_{xl}$. For a phantom network the transfer function can be approximated by the expression [11] $\Phi = \xi_{\text{sci}} f_{\text{mod}}/(1 + f_{xl})$, where ξ_{sci} is the fraction of the original chain segments that are modified by scissioning.

In the presence of the two networks Eq. (1) gets modified to

$$\sigma(\lambda) = G_0 \left[(1 - f'_{\text{mod}}) \left(\lambda^2 - \frac{1}{\lambda} \right) + f'_{xl} \left(\frac{\lambda^2}{\lambda_1^2} - \frac{\lambda_1}{\lambda} \right) \right], \quad (2)$$

where G_0 is the shear modulus of the virgin material. The shear modulus G in Fig. 2 (corresponding to a single network situation, i.e., $\lambda_1 = 1$) can be expressed as

$$G = G_0(1 - f'_{\text{mod}} + f'_{xl}) = G_0(1 - f_{\text{mod}} + f_{xl}). \quad (3)$$

The linear behavior of Fig. 2 can be expressed by the relation

$$\Delta f_{xl} = f_{xl} - f_{\rm mod} = f'_{xl} - f'_{\rm mod} = C_0 D, \qquad (4)$$

where Δf_{xl} is the net increase in cross-link density, and the constant $C_0 \sim 0.054$ (Mrad)$^{-1}$. Equation (4) is in good quantitative agreement with recent solvent swelling data on the same material [16]. Equation (2) solved for $\sigma(\lambda) = 0$ yields the following expression for recovered length λ_s:

$$\lambda_s = \left(\frac{1 + f_{\rm eff}\lambda_1}{1 + f_{\rm eff}/\lambda_1^2}\right)^{1/3}, \qquad (5)$$

where $f_{\rm eff} = f'_{xl}/(1-f'_{\rm mod})$. Equation (5) can be inverted to solve for $f_{\rm eff}$ for every experimental value of λ_s in Fig. 3. This yields the values displayed as symbols in Fig. 4 (top), which shows that the dependence of $f_{\rm eff}$ on λ_1 is weak and nonsystematic [17]. It is thus natural to construct a model in which $f_{\rm eff}$ is a function of D only [solid curve in Fig. 4 (top)], from which one can solve for the effective fractions of new cross-links f'_{xl} and of modified original chains $f'_{\rm mod}$, as displayed in Fig. 4 (bottom).

It is interesting to consider the small D limit (5 Mrad or lower) where the transfer function Φ is small and the effective fractions f'_{xl} and $f'_{\rm mod}$ are almost equal to f_{xl} and $f_{\rm mod}$, respectively. In this region we observe linear behavior: $f_{xl} \sim C_{xl} D$ and $f_{\rm mod} \sim C_{\rm mod} D$, where $C_{xl} = 0.114$ and $C_{\rm mod} = 0.060\,{\rm Mrad}^{-1}$, respectively. Let us try to interpret this in terms of molecular-level cross-linking and chain-scission events. Under cross-linking the number of new chain segments is

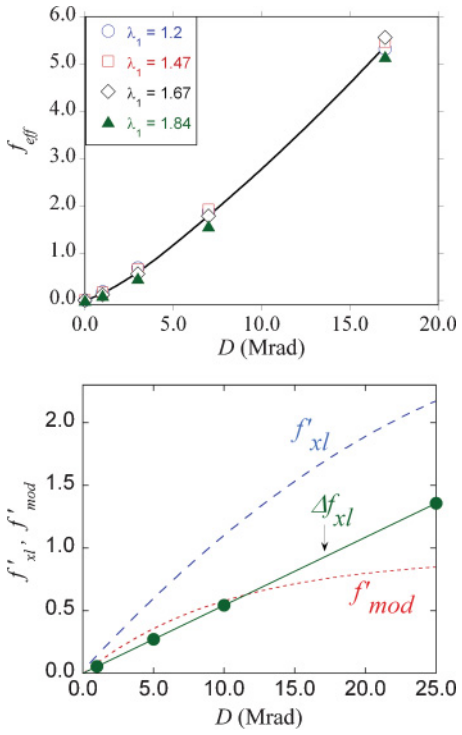

FIG. 4. (Color online) (top) Values of $f_{\rm eff} = f'_{xl}/(1 - f'_{\rm mod})$ from the λ_s data using Eq. (5), showing weak dependence on λ_1; solid line is the best (λ_1 independent) fit as a function of radiation dosage (D). (bottom) Effective fractions $f'_{xl}, f'_{\rm mod}$, and $\Delta f_{xl} = f'_{xl} - f'_{\rm mod}$ plotted separately. See text for the definitions of various symbols.

exactly *twice* the number of original chain segments that get modified; i.e., either two original chain segments cross-link into four new segments (*fourfold-connected* cross-links), or one original segment get cross-linked to a filler surface somewhere in the middle, leading to two new segments [18]. On the other hand, chain scission leads to mobile, often volatile, small-chain or molecular fragments, or to dangling bonds that can either (i) remain dangling or form a loop onto itself, or reconnect (ii) to a different dangling bond, (iii) to a filler surface, or (iv) to another chain segment somewhere in the middle (*threefold-connected* cross-links). Processes (iii) and (iv) lead to new chain segments twice that of the originally modified segments, processes (ii) yield the *same* number of segments as the original (i.e., no *net* change in the total number of cross-links), while processes (i) lead to a *decrease* in the net number of cross-links. *The fact that the ratio* $C_{xl}/C_{\rm mod} = 0.114/0.060$ *is close to* 2 *indicates that scission events of type (i) and (ii) are rare at low radiation dosages.*

Now we show that the behavior of $f'_{\rm mod}$ as shown in Fig. 4 (bottom) can be derived from the assumption that any monomer in the system has the same probability of modification (cross-linking or scission). For simplicity we consider the case of $\lambda_1 = 1$ (i.e., single network) where $f'_{\rm mod} = f_{\rm mod}$. We need to recognize that not all chains are of the same length, but rather the chain length between cross-links, henceforth expressed in terms of the number of monomers p, follows a statistical distribution, i.e., the MWD. Let $\tilde{n}(p, D)$ be the number of chain segments of length p monomers between cross-links for a sample exposed to a cumulative radiation dosage D. Thus the total number of monomers N in the system (which is independent of D) and the average chain length $p_{\rm av}(D)$ are, respectively, given by

$$N = \sum_p p\tilde{n}(p,D) \quad \text{and} \quad p_{\rm av}(D) = N \Big/ \sum_p n(p,D).$$

Assuming a constant rate of modification $r_{\rm mod}$ per monomer per unit radiation dosage the probability that an original chain of length p has been modified after exposure to a (cumulative) radiation dosage D is $1 - \exp(-r_{\rm mod} p D)$. This yields the following expression for $f_{\rm mod}$:

$$f_{\rm mod} = \sum_p [1 - \exp(-r_{\rm mod}\, pD)]\tilde{n}(p,0) \Big/ \sum_p \tilde{n}(p,0). \qquad (6)$$

For small D, expanding the exponential in Eq. (6) yields $f_{\rm mod} \approx r_{\rm mod}\, p_{\rm av}(0) D$, where $p_{\rm av}(0)$ is the average chain length between cross-links for the virgin material. Thus, $r_{\rm mod}\, p_{\rm av}(0) = C_{\rm mod} \sim 0.060\,{\rm Mrad}^{-1}$. Using this result in Eq. (6) along with the experimentally determined MWD for the virgin material (see below) yields a curve of $f_{\rm mod}$, in excellent agreement with Fig. 4 (bottom).

V. ^{1}H MULTIQUANTUM NMR MEASUREMENTS

In order to experimentally determine the MWD between junctions and restraints, we utilized the technique of ^{1}H multiquantum nuclear magnetic resonance (MQ-NMR) [19], which allows for the quantification of dipolar couplings between protons not averaged to zero due to rapid, but anisotropic, motion of the polymer chains. The anisotropic

dynamics are due to physical and chemical restrains (due to cross-links and entanglements, respectively). Recent work [20,21] has established that MQ-NMR-based quantification of the residual dipolar couplings in silicone elastomers is very robust, with the following relationship between the residual dipolar coupling (Ω_d) and the number of statistical segments between cross-links (p):

$$\frac{\langle \Omega_d \rangle}{\langle \Omega_0 \rangle} = \langle P_2(\cos\alpha) \rangle \frac{3r^2}{5p}, \tag{7}$$

where $\langle\,\rangle$ denotes averaging over all chain orientations, Ω_0 is the dipolar coupling in the absence of motion (preaveraged by the fast motion of the methyl group), P_2 is the second-order Legendre polynomial, α is the angle between the dipolar vector and the chain axis (i.e., the angle between the backbone chain axis and the Si-C vector), and r is the length of the end-to-end vector, $|\mathbf{R}|$, expressed as a ratio to that of the unperturbed melt,$|\mathbf{R}_0|$,i.e., $r = |\mathbf{R}|/|\mathbf{R}_0|$. Taking the number of monomers in a statistical segment to be 5.7 [22], the distribution $\tilde{n}(p, D)$ can be determined from MQ-NMR measurements using Eq. (7). Figure 5 displays the MQ-NMR spectra for the virgin material as well as for samples exposed to various radiation dosages. The intensity (y axis) is proportional to the number of monomers in each chain segment, i.e., $p\tilde{n}(p, D)$. Thus the area under each curve is proportional to N, the total number of monomers in the system. It is convenient to define a normalized MWD $n(p, D) = \tilde{n}(p, D)/N$, such that a normalized NMR intensity is equal to $pn(p, D)$, and the total area under each curve is 1. All curves in Fig. 5 (i.e., for each D) are normalized in this way.

The distribution in Fig. 5 represents the main MWD within the pure polymer part. In addition we also see a much weaker peak at smaller chain lengths ($p < 20$) that is likely associated with the silica fillers and/or resins inherent in the TR-55 formulation. Weak dipolar coupling at frequencies above 80 Hz can lead to significant uncertainties in the values of $n(p, D)$ at large values of p (>300 or so), thus leading to uncertainty in the peak *heights* (especially for $D \sim 10$ Mrad or below). However, the peak *positions* are robust, as we verified through multiple measurements. Figure 5 displays a monotonic shift of the MWD to smaller chain lengths and gradual narrowing of the peak as a function of increasing radiation. More specifically, with increasing D the average chain length $p_{\rm av}(D)$ decreases such that the cross-link density $\Delta f_{xl} = p_{\rm av}(0)/p_{\rm av}(D) - 1$ increases linearly in a manner quantitatively consistent with Eq. (4) (see Fig. 5 inset).

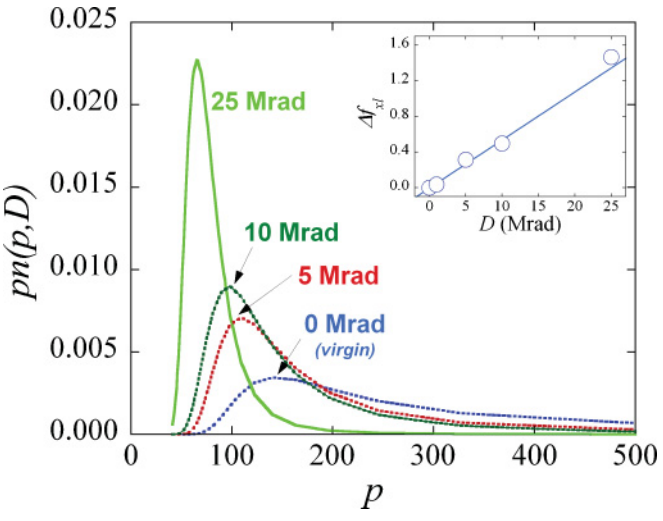

FIG. 5. (Color online) MWD [$pn(p, D)$] from MQ-NMR measurements for various radiation dosages. Inset: Corresponding chain density increment: $\Delta f_{xl} = p_{\rm av}(0)/p_{\rm av}(D) - 1$ as a function of D; solid curve: $y = C_0 D$; see Eq. (4).

VI. MESOSCALE NETWORK SIMULATIONS

To simulate the above radiation-induced evolution of MWD, and more specifically to decipher the dominant underlying molecular-level changes in the network, we employed a coarse-grained, mesoscopic polymer network model that has been previously applied to a similar PDMS material [23]. The model consists of a set of cross-link nodes (i.e., junctions) connected via single finite extensible nonlinear elastic (FENE) bonds (that can be potentially cross-linked and/or scissioned), which represent the chain segments between cross-links. In addition, there is a repulsive Lennard-Jones interaction between all cross-link positions to simulate volume exclusion effects. Since we are concerned only with the polymer network, the filler particles are not explicitly incorporated into the model.

The first step was to create a network that resembles the virgin distribution of Fig. 5. To this end, we placed more than 4000 random "nodes" (representing junctions) in a three-dimensional cubic box with periodic boundary conditions. Pairs of junctions within a chosen cutoff were then randomly connected by FENE bonds. The Lennard-Jones and FENE interaction parameters were adjusted and the degree of polymerization (p) for a given length of a FENE bond calibrated until the MWD computed from our network matched the experimental MWD of the virgin material.

To simulate the radiation-induced evolution of the above network, we first considered the situation with only cross-linking and no scissioning (i.e., only fourfold connections). For this, we created the virgin network with only fourfold-connected junctions and performed additional random cross-link operations between FENE bonds (i.e., segments) in accordance with Δf_{xl} values given by Eq. (4). We added new cross-links in radiation dosage steps of 1 Mrad and at each step structurally optimized (i.e., relaxed) the new network using the LAMMPS code [24].

Figure 6 displays the simulated evolution of MWD of the above network (red curve) under fourfold coordination for four different radiation dosages along with the experimental data (blue line). We also considered the MWD evolution when all new cross-links were threefold connected (i.e., scission induced), as shown by green dashed lines. The differences in MWD between fourfold and threefold connected cases are negligible, and both mechanisms lead to excellent agreement in the peak positions as compared to NMR data. The differences between peak heights, especially for $D \leqslant 10$ Mrad, are not surprising given the uncertainty in the NMR data in the long-tail part (see discussion above; Fig. 5). However at 25 Mrad, the disagreement between the experimental and simulated data is significant and points to effects not considered in

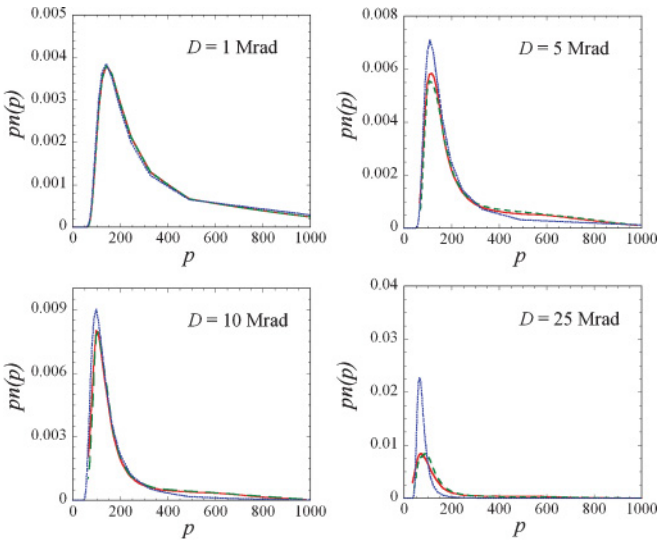

FIG. 6. (Color online) Comparison of experimental MWD of Fig. 5 (blue line) with computed MWD for fourfold linking only (red solid line) and threefold linking only (green dashed line).

the simulations. To explain such differences, we performed simulations in which we allowed for the presence of dangling bonds (and/or loops), which did not form junctions. This leads to simulated peaks being narrower and higher, closer to the NMR data. Similar effects could also be expected from the creation of volatile small-chain fragments.

VII. SUMMARY

In summary, the present work demonstrates that the exposure of elastomeric rubber materials to controlled dosages of radiation can alter mechanical properties in a reproducible and predictable manner. The newly developed technique of multiquantum NMR enables accurate characterization of MWD between cross-links (or physical restraints), which along with a simple, yet elegant network model and mesoscale simulations provides useful insights into radiation-induced modifications at the molecular level. For our specific rubber material the NMR data up to 10 Mrad appear consistent with either fourfold- or threefold-connected junctions, with the presence of dangling bonds, loops, or small volatile species becoming possibly important at much higher dosages. Experimental control and insights such as these can be hoped to create novel opportunities and applications in the field of radiation-controlled manipulation of material properties.

ACKNOWLEDGMENTS

This work was performed under the auspices of the US Department of Energy by Lawrence Livermore National Laboratory under Contract DE-AC52-07NA27344.

[1] J. E. Mark, B. Erman, and F. R. Eirich, eds., *Science and Technology of Rubber* (Academic Press, New York, 2005).
[2] C. A. Harper, ed., *Handbook of Plastics, Elastomers, & Composites* (McGraw-Hill, New York, 2002).
[3] A. Ciesielski, *An Introduction to Rubber Technology* (Rupra Technology, Totton, Southampton, UK, 1999).
[4] A. S. Palsule, S. J. Clarson, and C. W. Widenhouse, J. Inorg Organomet. Polym. **18**, 207 (2008).
[5] A. V. Tobolsky, *Properties and Structure of Polymers* (John Wiley, New York, 1960).
[6] J. G. Curro and E. A. Salazar, J. App. Polym. Sci. **19**, 2571 (1975).
[7] J. A. Shaw, A. S. Jones, and A. S. Wineman, J. Mech. Phys. Solid **53**, 2758 (2005).
[8] B. Erman and J. E. Mark, *Structures and Properties of Rubber-like Networks* (Oxford University Press, Oxford, 1999).
[9] L. R. G. Treloar, *The Physics of Rubber Elasticity* (Clarendon Press, Oxford, 1975).
[10] D. R. Rottach *et al.*, Macromolecules **40**, 131 (2007).
[11] H. S. Fricker, Proc. R. Soc. Lond. A **335**, 269 (1973).
[12] Neo-Hookean is the simplest model and applicable for not-too-large strains. For larger strains one needs to use more sophisticated models. See, e.g., Ref. [9].
[13] Permanent set (P_s), a commonly used term in this context, is related to λ_s through the equation $P_s = (\lambda_s - 1)/(\lambda_1 - 1)$.
[14] The permanent set measurements reported here were performed prior to any stress-strain cycling, and therefore do not include possible hysteresis effects.
[15] A. V. Tobolsky, I. V. Prettyman, and J. H. Dillon, J. App. Phys. **15**, 380 (1944); R. D. Andrews, A. V. Tobolsky, and E. E. Hanson, *ibid.* **17**, 352 (1946).
[16] R. S. Maxwell *et al.*, Polym. Degrad. Stab. **94**, 456 (2009).
[17] The $\lambda_1 = 1.84$ branch in Fig. 4 (top) might indicate possible λ_1-dependence of f_{eff} at larger values of λ_1. However, to establish such trends with certainty more experiments are necessary. Here we ignore any such dependence.
[18] In this discussion we are neglecting the formation of rings through cross-linking of the same chain segment folded onto itself.
[19] K. Saalwächter, J. Am. Chem. Soc. **125**, 14684 (2003).
[20] K. Saalwächter *et al.*, J. Chem. Phys. **119**, 3468 (2003).
[21] J. R. Giuliani *et al.*, J. Phys. Chem. B **111**, 12977 (2007).
[22] W. Kuhn and F. Grün, Kolloid-Z. **101**, 248 (1942).
[23] T. H. Weisgraber *et al.*, Polymer **50,** 5613 (2009).
[24] LAMMPS: Large-scale Atomic/Molecular Massively Parallel Simulator; see [http://lammps.sandia.gov].